THE JOURNAL OF PHYSICAL CHEMISTRY C

Article

pubs.acs.org/JPCC

Aggregation-Induced Enhancement Effect of Gold Nanoparticles on Triplet Excited State

Wen Yang, Kunhui Liu, Di Song, Qian Du, Rennian Wang, and Hongmei Su*

Beijing National Laboratory for Molecular Sciences (BNLMS), State Key Laboratory of Molecular Reaction Dynamics, Institute of Chemistry, Chinese Academy of Sciences, Beijing 100190, China

Supporting Information

ABSTRACT: Remarkable optical properties are posed with gold nanoparticles (AuNPs) due to the excitation of localized surface plasmon resonances, which makes AuNPs affect strongly both the ground state and the excited state of adjacent organic molecules. Compared with the ground state, the effect of AuNPs on excited state of organic molecules is not always fully understood. Here, we performed transient UV−vis absorption experiments to monitor the triplet excited state formation of three cationic dyes and one anionic dye in the presence of two types of gold nanoparticles: the citrate-stabilized AuNPs and ATP-protected AuNPs. It is found that the three cationic dyes can cause efficient aggregation of citrate-stabilized AuNPs, leading to AuNPs aggregates with varied size, whereas the ATP-protected AuNPs can be sustained in the monodispersed state. By comparing the circumstances of aggregated AuNPs and monodispersed AuNPs, we demonstrate that the enhancement effect on triplet excited state formation results from the aggregation of gold nanoparticles and depends on the aggregation size. These findings reveal the aggregation induced plasmon field interaction of AuNPs with excited state population dynamics and may enable new applications of aggregated metal nanoparticles, where aggregates can serve as stronger plasmonic nanoantennas.

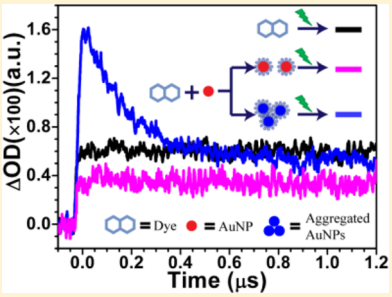

INTRODUCTION

Metal nanoparticles have emerged as one of the most exciting areas of scientific research in the past several decades due to its unique optical, electronic, chemical, and magnetic properties.[1] Excitation of the metal nanoparticle leads to a strong absorption band in the UV−vis to near-infrared region, which is originated from coherent oscillations of conduction electrons excited by electromagnetic radiation known as localized surface plasmon resonances (LSPRs), and this absorption band can be tuned by altering the size, shape, and surroundings of the nanoparticle.[2] Metal nanoparticles can strongly interact with the adjacent organic molecules due to their LSPRs.[3] These interactions are displayed in a variety of ways, including electron transfer from the photoexcited organic dyes to the metal nanoparticles,[4] energy transfer from metal nanoparticles to surrounding molecules,[5,6] and influence on both radiative and nonradiative deactivation processes of excited states of organic molecules.[7] These remarkable interactions make metal nanoparticles ideal for use in surface-enhanced Raman spectroscopy (SERS),[8,9] surface-enhanced fluorescence (SEF),[10] solar cells,[11] and medical therapeutics.[12] A better understanding of the interactions between metal nanoparticles and organic molecules will enable effective utilization of metal nanoparticles for various applications.

Normally, organic molecules are brought into the proximity of metal nanoparticles through covalent binding or noncovalent binding. In the former case, organic molecules or metal nanoparticles are modified and bind together through functional groups,[13] such as amines, thiols, isothiocyanates, and silanes, etc., while in the latter case both organic molecules and metal nanoparticles are unmodified and the binding occurs through electrostatic interaction or van der Waals force. For the noncovalent binding interactions between metal nanoparticles and small molecules, it was found that the ground state UV−vis absorption of a number of cationic thiazine dyes, such as methylene blue (MB) and toluidine blue, can be enhanced up to 10-fold by gold nanoparticles (AuNPs), when bounded to the surface of AuNPs through electrostatic attraction.[14] The enhancement effect is not limited to ground state. Interestingly, the formation of triplet excited state of methylene blue (^{3}MB*) was observed to be enhanced by the photochemically prepared AuNPs, when the surface was largely unprotected.[15] A transmitter−receiver antenna model was proposed,[15] where the AuNPs served as antenna, enhancing the light absorption of receiver MB such that an increased population of dye excited singlet and then triplet state was resulted. Both of these two instances mentioned the possible aggregation of AuNPs, which can result from the charge neutralization between cationic dyes and negatively charged AuNPs.

The optical properties of aggregated nanoparticles show complex plasmonic resonance and significant deviation from monodispersed nanoparticles.[16,17] Aggregation will lead to the strong coupling of nanoparticle surface plasmons between neighboring nanoparticles[18] and results in ordered multiscale

Received: October 20, 2013
Revised: December 8, 2013
Published: December 9, 2013

   dx.doi.org/10.1021/jp410369w | J. Phys. Chem. C 2013, 117, 27088−27095

organization toward the specific nano-optical functionalities[19] as well as in new physical and chemical properties.[20] For instance, previous studies have demonstrated that the aggregated nanoparticles exhibit exciting SERS performance[21,22] and better SERS enhancement factor than monodispersed nanoparticles.[8] Because of the strong interparticle coupling, aggregated nanoparticles may play an important role in electromagnetic enhancement and thus have a significant influence on excited state population dynamics, which remains untangled yet.

Here, in this work, we performed transient UV−vis absorption experiments to monitor the triplet excited state formation of three different cationic thiazine dyes and one anionic dye (molecular structures shown in Scheme 1) in the presence of AuNPs that were synthesized by the Turkevich citrate reduction method. Under current experimental conditions, the cationic dyes efficiently induced AuNPs to aggregate upon mixing with negatively charged AuNPs. To prevent aggregation and ensure monodispersion, AuNPs were protected by the efficient surface-stabilization agent adenosine triphosphate (ATP). By comparing the circumstances of aggregated AuNPs and monodispersed AuNPs, we show that the plasmon enhancement effect on triplet excited state formation does not occur for monodispersed AuNPs but is significant for aggregated AuNPs, and the enhancement effect is highly correlated with the aggregation size and degree. These findings reveal the aggregation-induced plasmon effect of AuNPs on excited state population dynamics and may enable new applications of aggregated metal nanoparticles.

Scheme 1. Molecular Structure of MB, Azure A, Thionine, and RB

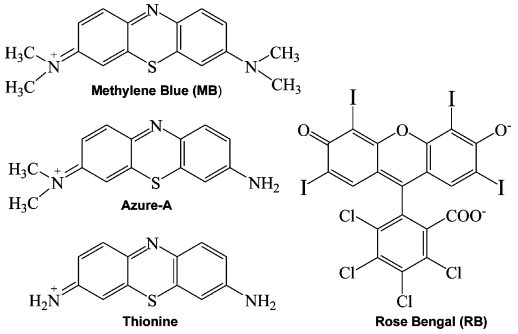

MATERIALS AND METHODS

Materials. Methylene blue, azure A, thionine, and Rose Bengal were purchased from Sigma-Aldrich and used without further purification. Adenosine triphosphate (ATP) solution was purchased from Beijing BioDee Bio Tech Corporation Ltd. All glassware was cleaned in freshly prepared aqua regia solution (HCl/HNO_3 = 3:1) and then rinsed by double distilled water. $HAuCl_4 \cdot 3H_2O$ and trisodium citrate at analytical grade were purchased from Sinopharm Chemical Reagent Beijing Corporation Ltd. and used without further purification. Ultrapure water (18.2 MΩ, purified by Millipore filtration) was used for all synthesis and solution preparations.

Synthesis of Gold Nanoparticles. Solution of gold nanoparticles was prepared according to typical method, as described by Turkevich[23] and Frens.[24] In brief, 143 mL of aqueous $HAuCl_4$ (2.8×10^{-4} M) was prepared in a 250 mL round-bottom flask. The solution was brought to boiling. Under vigorous stirring, 7 mL of 38.8 mM aqueous sodium citrate was added quickly. Then the solution underwent a series of color changes before finally reached a red wine color. The

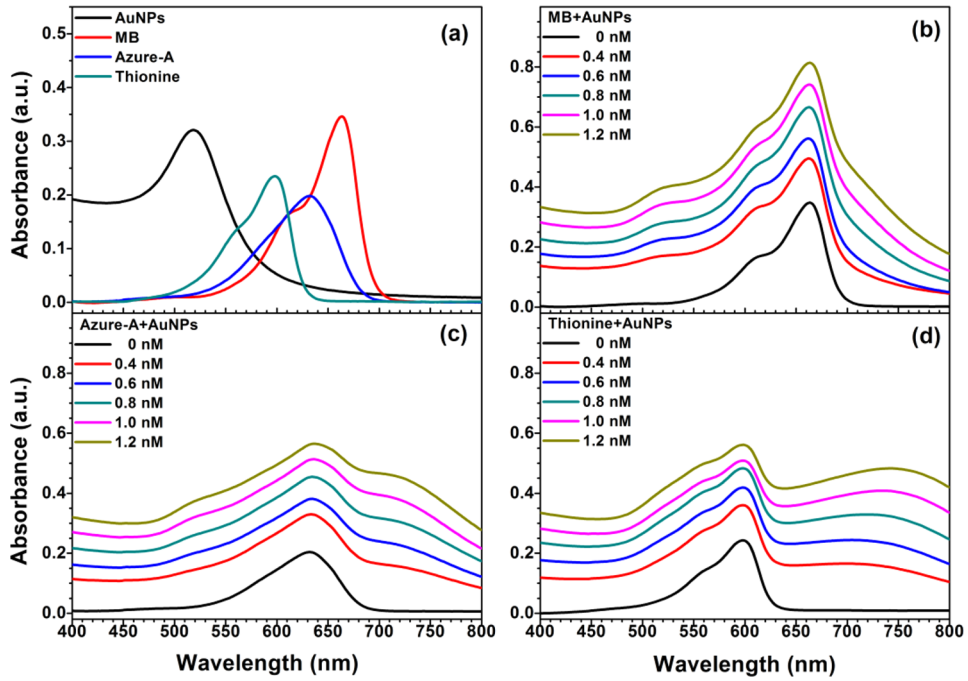

Figure 1. (a) UV−vis spectra for pure sample of AuNPs (0.6 nM) and three cationic dyes (5 μM) in aqueous solution. (b−d) UV−vis absorption spectra for the mixed solutions of 5 μM (b) MB, (c) azure A, and (d) thionine with different concentrations of AuNPs. The dye spectra fall in between the two plasmon bands: the 520 nm band for individual AuNPs and the 700−800 nm band for aggregated AuNPs. The background absorption formed by the two plasmon bands increases with the AuNPs concentration, on top of which the enhanced dye absorption spectra are superimposed.

dx.doi.org/10.1021/jp410369w | J. Phys. Chem. C 2013, 117, 27088−27095

solution was kept boiling and stirring for 15 min and was then cooled to room temperature. The prepared gold solution consists of dispersed spherical particles with a mean diameter of 15 ± 2 nm according to TEM characterization. The concentration of the prepared gold solution was estimated to be 2.2 nM based on the size of nanoparticles, the amount of starting materials, and the final volume of stock solution.

Transmission Electron Microscopy Measurement. TEM observations were carried out with a 300 keV Tecnai F30 transmission electron microscope. The TEM sample was prepared by dropping gold solution onto a copper grid.

Steady-State Spectral Measurements. Ground state absorption spectra were recorded with a UV−vis spectrometer (model U-3010, Hitachi). Quartz cuvettes of 1 cm path length were used for all absorption measurements. For each of the dyes, six samples were prepared in glassware cuvettes. In the sample solutions, the dye concentration was fixed at 5 μM; when mixed with AuNPs, the AuNPs concentration was varied from 0.4 to 1.2 nM in 0.2 nM steps by mixing AuNPs stock solution with ultrapure water, to give a final volume of 3.0 mL. When AuNPs were protected by ATP, they were mixed with ATP in a 1:1000 molar ratio for 5 min incubation at room temperature. Each mixture was shaken and equilibrated at room temperature for 1 min to ensure good mixing before the measurement.

Laser Flash Photolysis. The transient UV−vis spectra and triplet state kinetics were measured by nanosecond time-resolved laser flash photolysis (LFP) setup that has been described previously.[25,26] Briefly, the instrument comprises a Edinburgh LP920 spectrometer (Edinburgh Instrument Ltd.) combined with an Nd:YAG laser (Surelite II,Continuum Inc.). The excitation wavelength is 532 nm laser pulse from Q-switched Nd:YAG laser (1 Hz, fwhm ≈7 ns, 10 mJ/pulse). The analyzing light was from a 450 W pulsed xenon lamp. A monochromator equipped with a photomultiplier for collecting the spectral range from 350 to 850 nm was used to analyze transient absorption spectra. The signals from the photomultiplier were displayed and recorded as a function of time on a 100 Hz (1.25 Gs/s sampling rate) oscilloscope (Tektronix, TDS 3012B), and the data were transferred to a personal computer. Data were analyzed by the online software of the LP920 spectrophotometer. The fitting quality was judged by weighted residuals and reduced χ^2 value. Sample solutions were freshly prepared for each measurement. Quartz cuvettes of 1 cm path length were used for all LFP measurements. All LFP experiments were performed in N_2-saturated solution.

RESULTS AND DISCUSSION

The synthesized gold nanoparticles (15 nm) were first characterized by UV−vis absorption spectroscopy (Figure 1) and transmission electron microscopy (Figure S1, Supporting Information). As shown in Figure 1a, the pure sample of AuNPs exhibits the characteristic plasmon resonance peak for monodispersed particles at 520 nm. In addition, individual AuNPs with spherical shape and being separated from each other can be clearly seen in the TEM image (Figure S1a). Synthesized by the Turkevich citrate reduction method, the citrate-stabilized AuNPs are negatively charged and may form large clusters or aggregates upon addition of cationic dyes due to charge neutralization,[13,27] causing a large and rapid change in the ground state absorption spectra for cationic dyes.[28,29]

As seen in the UV−vis absorption spectra (Figure 1a), pure samples of the three cationic dyes (MB, azure A, and thionine) exhibit characteristic absorption bands at 660, 630, and 600 nm, respectively. Upon addition of AuNPs, significant changes were observed (Figure 1b−d). Figure 1b shows the absorption spectra of MB with addition of AuNPs at various concentrations. Compared with the spectrum for pure MB, the addition of AuNPs to MB results in enhancement in the absorption intensity and broadening of absorption band. With the addition of 1.2 nM AuNPs, the MB absorbance at maxima (660 nm) is enhanced nearly 2.4 times, after deducting the background absorbance of AuNPs. Such absorption enhancement and spectral broadening become more obvious with the increasing of AuNPs concentration. On top of the MB spectra, the plasmon band for monodispersed AuNPs at 520 nm is present. As the concentration of AuNPs increases, a broad band between 700 and 800 nm can be discerned, and it red-shifts at increased AuNPs concentrations, indicating the occurrence of aggregation.[29−31] Moreover, the TEM image reveals the occurrence of AuNPs aggregation upon addition of MB. As shown in Figure S1b, the AuNPs form close-packed nanoclusters, which are composed of 2−6 nanoparticles.

Similar to MB, the addition of AuNPs to the dye solution of azure A or thionine also leads to enhanced absorption and broadening of spectral bands (Figure 1c,d). Compared with pure azure A and thionine, the absorbances at 630 and 600 nm are increased ∼2.5 and ∼2.0 times, respectively, when mixed with 1.2 nM AuNPs solution. In contrast to the system of MB, the AuNPs aggregation is more noticeably seen in the dye solution of azure A or thionine, as manifested by the obvious presence of the broad band between 700 and 800 nm, and its red-shift with increased AuNPs concentration, which is a typical indication of aggregation.[29−31] The TEM images (Figure S1c,d) coincide with the spectral results, showing clearly the aggregation. When mixed with azure A, AuNPs form also close-packed nanoclusters consisting of 6−10 nanoparticles, larger than the MB case. While in the thionine solution, AuNPs form large linear aggregate, which consists of tens of nanoparticles. According to the UV−vis spectra and TEM images, the size or degree of AuNPs aggregation in the presence of different cationic dyes should follow the order of thionine > azure A > MB.

Previously, Guo and co-workers have reported that 5 and 18 nm negatively charged AuNPs can form 45 and 84 nm aggregates, respectively, when adsorbed with thionine.[28] Chegel and co-workers have found that organic compounds containing thiol or amine groups, such as azure A or thionine, can strongly promote the aggregation of citrate-stabilized AuNPs.[29] These studies are comparable with our results and further support the aggregation that we observed. Moreover, it should be noted that when the aggregation is induced by electrolytes, such as KCl and NaCl, the nanoparticles are usually fused together due to the collapse of electrical double layers.[31] In contrast, the nanoclusters or aggregates are almost individually isolated when they are induced by organic molecules.[28,29] This is why the aggregates that we observed in TEM images are separated from each other.

The ground state UV−vis absorption spectra not only provide compelling evidence that these cationic dyes lead to aggregation of AuNPs but also show that the ground state absorption of cationic dyes can be enhanced by AuNPs. Presumably, the enhanced ground state absorbance obtained for the cationic dyes could most readily result from the electromagnetic enhancement brought by gold nanoparticles. An interesting question emerges then. Would such effects also

act on the excited states of dye molecules, leading to different population dynamics in the presence of AuNPs? To explore this issue, we monitored the transient absorption of triplet excited state for the three cationic dyes in the absence and presence of AuNPs after 532 nm laser excitation by laser flash photolysis.

In the nanosecond time-resolved UV−vis absorption spectra, the citrate-stabilized AuNPs alone do not give a signal under 532 nm laser excitation because the AuNPs excitation signal has been quenched completely at this time scale. For the three cationic dyes, transient absorptions due to their triplet excited states are present around 420 nm (transient absorption spectra for the three dyes are shown in Figure S2). Therefore, the decay behavior at 420 nm was monitored for ^{3}MB*, ^{3}azure A*, and ^{3}thionine*, respectively. In the absence of AuNPs, the decay process can be reasonably fit with a single exponential, and the lifetimes of ^{3}MB*, ^{3}azure A*, and ^{3}thionine* are 88 ± 1.5, 69 ± 0.7, and 61 ± 0.6 μs, respectively, which are fairly long-lived (Figure S3). Hence, no decay tendency is displayed in the temporal curves at short time scales of 1.2 μs for the pure dye samples (black curves in Figure 2).

In contrast, a biexponential is required to fit the decay kinetics in the presence of AuNPs, as shown with the temporal traces in both the short (Figure 2) and long time scales (Figure S3). For each of the three cationic dyes, the decay kinetics of the triplet excited states shows a short decay component at the initial 0.4 μs and then is followed by a long decay process. In addition, the short decay component is accompanied by significant changes in the intensity of transient absorbance. In the presence of 0.6 nM and 1.2 nM AuNPs, the transient absorbance of ^{3}MB* at initial formation time is 2 and 2.5 times enhanced, respectively, compared with that in the absence of AuNPs (Figure 2a). Traces at different AuNPs concentrations reveal that while the signal amplitude due to the fast decay depends on the AuNPs concentration, the lifetime of short decay component (τ = 80 ± 10 ns) is largely unchanged. For ^{3}azure A*, the transient absorbance is displayed with ∼1.8 times enhancement at initial formation time in the presence of 1.2 nM AuNPs (Figure 2b). The enhancement factor for ^{3}azure A* is less than that for ^{3}MB*. Like the decay of ^{3}MB*, the short decay component (τ = 90 ± 5 ns) is only observed in the presence of AuNPs. But quenching was also observed, as seen by the decreased absorbance intensity lower than that of pure ^{3}azure A* after 0.4 μs.

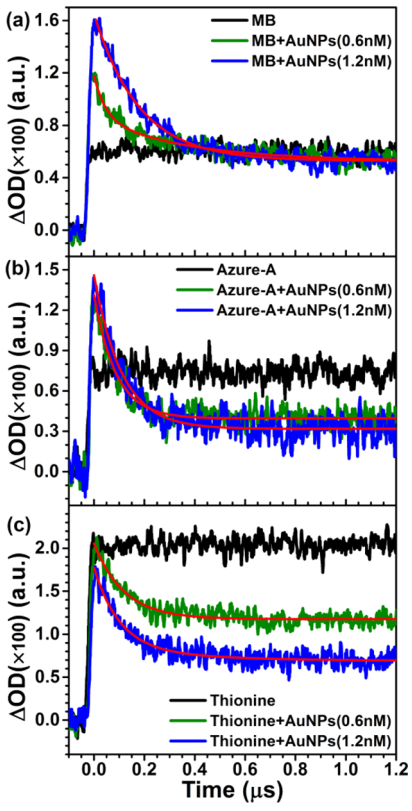

Figure 2. Decay kinetics of transient absorption at 420 nm for the triplet excited states (a) ^{3}MB*, (b) ^{3}azure A*, and (c) ^{3}thionine* after 532 nm laser excitation of the dye solution (5 μM) in the absence and presence of different concentrations of AuNPs. The temporal traces are displayed in short time scales (1.2 μs) to make the signal amplitude enhancement clearly seen, while long time scale traces are displayed in Figure S3. Red colors curves represent double-exponential fitting results for the decay traces of dye triplets in the presence of AuNPs.

Since the ground state absorption spectra for the third dye, thionine, show considerable overlap with the plasmon band of AuNPs (Figure 1a), it is naturally to hypothesize that the triplet excited state ^{3}thionine* could be markedly enhanced by AuNPs due to plasmon resonance. However, for ^{3}thionine*, although the short decay component (τ = 80 ± 5 ns) can also be observed, the signal amplitude of the transient absorbance does not show any enhancement in the presence of AuNPs (Figure 2c). Instead, after the short decay, the intensity of transient absorbance of ^{3}thionine* is markedly lower than that in the absence of AuNPs.

For the three cationic dyes, the presence of AuNPs has enhanced the transient absorbance of ^{3}MB* and ^{3}azure A* at initial formation time but does not exhibit enhancement effect on ^{3}thionine*, although thionine has ground state absorption partially in resonance with the 520 nm plasmon band of AuNPs. This result indicates that the effect of AuNPs on triplet excited state formation is not correlated with the plasmon optical resonance but tends to be related to other mechanisms.

Plasmon field interactions, in particular, the transmitter−receiver antenna interaction, may provide interpretations.[15,32,33] Initially at laser excitation, AuNPs serve as antenna that can enhance the ground state absorption of dye molecule, resulting in enhancement in singlet excited state populations and then triplet populations after intersystem crossing (ISC). The cationic dyes adsorbed with AuNPs can be classified into three categories in terms of distance. The dye molecules bound to the surfaces of nanoparticles (the distance <2 nm) are subject to fast surface quenching of excited state populations, and there is no enhancement effect. For the dye molecules close to the surface at the distance of 2−20 nm, the enhancement effect is favored, but reaching surface for quenching is also easy and thus accelerated due to the static AuNPs quenching. Therefore, the short decay component and its enhanced intensity observed for the triplet excited states of cationic dyes in the presence of AuNPs (Figure 2) can be attributed to these molecules close to the surface. The third type is the remote dye molecules (the distance >20 nm), which are mostly unaffected by plasmon effects. For these molecules, their triplet excited state cannot be enhanced, but simply quenched when colliding with AuNPs, undergoing the dynamic quenching that accounts for the long decay component of temporal traces (Figure S3).

Short decay components were observed for all three cationic dyes, indicating that these three dye molecules are truly brought into the proximity of AuNPs and the plasmon field effect takes

dx.doi.org/10.1021/jp410369w | J. Phys. Chem. C 2013, 117, 27088−27095

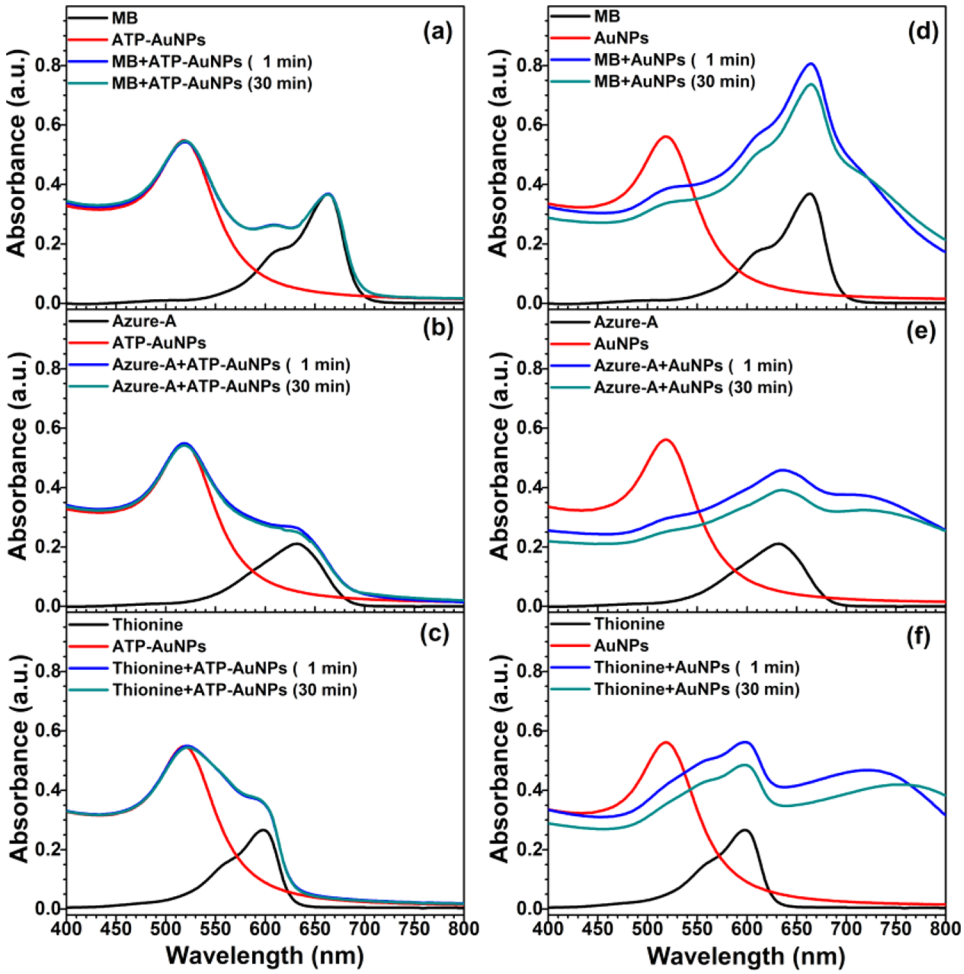

Figure 3. Left panel: UV−vis absorption spectra of 5 μM (a) MB, (b) azure A, and (c) thionine in the absence and presence of 1.2 nM ATP-protected AuNPs. Right panel: UV−vis absorption spectra of 5 μM (d) MB, (e) azure A, and (f) thionine in the absence and presence of 1.2 nM citrate-stabilized AuNPs.

place. But why do AuNPs display different effects for the three cationic dyes? The enhancement factors of AuNPs on the triplet yields follow the order of MB > azure A > thionine. Noticeably, this order is just the opposite of the aggregation degree of AuNPs caused by the three dyes. This leads to a postulation that the enhancement effect is linked to the AuNPs aggregation. To explore this issue, we performed well-controlled experiments of monodispersed AuNPs to compare with those already obtained for the aggregated AuNPs.

To prepare monodispersed AuNPs and prevent AuNPs aggregation caused by cationic dyes, we adopted the method of protecting citrate-stabilized AuNPs by the efficient surface-stabilization agent, adenosine triphosphate (ATP), before they were mixed with solutions of cationic dyes.[34−36] Unlike citrate-stabilized AuNPs, the ATP-protected AuNPs are even stable in the presence of high salt concentrations. The extremely high stability of the ATP-protected AuNPs may be due to the fact that nucleotide can bind to citrate-stabilized AuNPs with the displacement of weakly bound citrate ions,[36] so that more negatively charged phosphate groups increase the amount of negative charge on the surface of AuNPs.[34] This has been verified by surface charge measurements: the negative charge of ATP-protected AuNPs is greater than that of citrate-stabilized AuNPs.[36] Using the strategy of ATP-protected AuNPs, the cationic dyes can still be adsorbed to the surface of negatively charged AuNPs but will not cause AuNPs aggregation. Furthermore, the absorption band of ATP is in the wavelength range below 300 nm, which will not interfere with the dye spectra at visible range and will not be excited by 532 nm laser flash photolysis.

Ground state UV−vis spectra (Figure 3) were examined first to verify that the ATP-protected AuNPs are still in monodispersed state when mixed with cationic dyes. As clearly shown in Figure 3a−c for the three dyes after addition of 1.2 nM ATP-protected AuNPs, the spectra are simply the sum of the individual spectra of AuNPs and dyes. There are only the absorption bands due to the monodispersed AuNPs at 520 nm and dyes at longer wavelength. The typical 700−800 nm band representing AuNPs aggregation is not present, demonstrating that the ATP-protected AuNPs are still in monodispersed state when mixed with cationic dyes. Moreover, the dye spectra recorded at 30 min after addition of 1.2 nM ATP-protected AuNPs remain the same as that recorded after 1 min mixing, indicating the stability of the monodispersed state. In contrast, for the three dyes after addition of 1.2 nM citrate-stabilized AuNPs without being ATP-protected, the typical AuNPs aggregation band between 700 and 800 nm (Figure 3d−f) emerges, while the absorbance intensity of monodispersed band at 520 nm decreases in the spectra. After 30 min mixing, the spectra display essentially a decrease in intensity due to

dx.doi.org/10.1021/jp410369w | J. Phys. Chem. C 2013, 117, 27088−27095

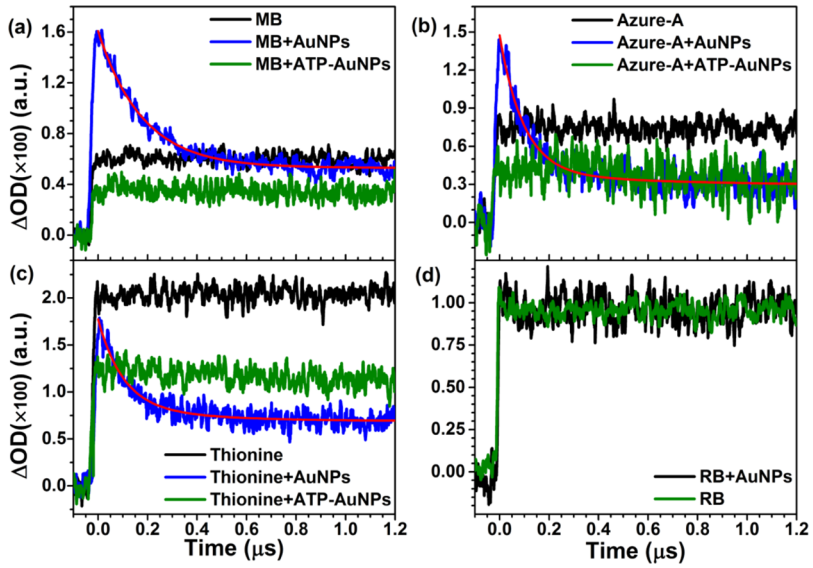

Figure 4. Decay kinetics of transient absorption at 420 nm for the triplet excited states of cationic dyes: (a) ^{3}MB*, (b) ^{3}azure A*, (c) ^{3}thionine*, after 532 nm laser excitation of the dye solution (5 μM) in the absence and presence of 1.2 nM AuNPs with ATP protection (green curves) and without ATP protection (blue curves). (d) Decay kinetics of transient absorption at 450 nm for the triplet excited state of the anionic dye ^{3}RB* in the absence and presence of 1.2 nM AuNPs. Red colors curves represent double-exponential fitting results for the decay traces of dye triplets in the presence of AuNPs without ATP protection. Decay of dye triplets by ATP-protected AuNPs is only visible at long time scale and their fitting results are displayed in Figure S4.

formation of AuNPs aggregation that subsequently precipitated. These results confirm that after mixing with cationic dyes the ATP-protected AuNPs remain in dispersed form, but the citrate-stabilized AuNPs undergo aggregation.

Interestingly, it shows here that when AuNPs are in the monodispersed state (Figure 3a–c), the ground state absorption intensities for the three cationic dyes are not enhanced at all, with their absorbance retaining the same intensity as individual dyes. The absorbance in the whole spectra range is simply the sum of the individual absorbance of AuNPs and dyes. This is very different from the case for the aggregated AuNPs (Figure 3d–f), which exhibit obvious enhancement for the ground state absorption intensities of the three cationic dyes.

Ground state UV–vis spectra indicate totally different effects of the monodispersed AuNPs from aggregated AuNPs. How would the dispersion state of AuNPs affect excited state? Similar transient UV–vis spectral measurements were performed for the three cationic dyes in the presence of the well-prepared monodispersed AuNPs to compare with those already obtained for the aggregated AuNPs. As shown in Figure 4, the transient absorption for the three triplet excited states, ^{3}MB*, ^{3}azure A*, and ^{3}thionine*, only exhibits quenching in intensity after adding1.2 nM ATP-protected AuNPs (the quenching is more noticeable at long time scale as shown in Figure S4), while the decay kinetics remains largely unchanged at the short time scale. Obviously, the short decay component accompanied by the enhanced triplet intensity for the aggregated AuNPs (also shown in Figure 4 for comparison) was not obtained for the monodispersed AuNPs. It shows here that the monodispersed AuNPs do not have enhancement effect on the triplet excited state yield of the three cationic dyes, consistent with the ground state results. Whether for ground or triplet excited state of cationic dyes, the absence of the enhancement effect from the monodispersed AuNPs, compared with the obvious enhancement effect from the aggregated AuNPs, is a strong indication that the nanoparticle dispersion state plays important roles in these processes.

To illustrate the important role of AuNPs aggregation, the relationship between the aggregated nanoparticles and the antenna effect should be considered. The plasmon antenna effect depends not only on size, shape, environment, and wave frequency of nanoparticles but also on the interparticle distance.[21,37] As a result of aggregation, the interparticle distance becomes shorter, and the shorter distances facilitate the formation of higher-order collective modes and strong surface plasmon coupling between neighboring nanoparticles because the interparticle coupling resulted from near-field is inversely proportional to d^3, where d is the distance between the neighboring nanoparticles.[38] Because of this strong interparticle coupling, aggregate can dramatically enhance its ability to concentrate electromagnetic energy.[18] Furthermore, the aggregated nanoparticles permit the formation of hot spots,[39] which dominate the nanoantenna system and is capable of supporting resonances and amplifying light in the near-field. For these reasons, the aggregated nanoparticles can act as better antenna. Recently, self-assembled nanoantennas have been used to obtain the better fluorescence enhancement.[40]

Our experimental results indicate a mechanism of aggregation induced plasmon field interaction for the enhancement of triplet excited state formation. When the nanoparticles are in monodispersed state, the antenna effect might not be strong enough to enhance the initial light absorption of receiver dye molecules so that no enhancement was observed for ground state absorption and subsequent triplet excited state formation. Whereas AuNPs aggregation results in stronger antenna effect and can greatly enhance the light absorption, leading to an increased population of excited singlet states. These in turn partition between surface quenching and ISC that yields triplet excited state. The triplet excited state is enhanced by antenna effect, while its decay becomes faster due to accelerated quenching. This is why a short decay component

was observed with the enhancement of triplet yields (Figure 2). However, the total enhancement factor for triplet excited state is the result of a balance between enhancement effect and surface quenching effect. Only when the enhancement effect is stronger than the quenching effect, the increased formation of triplet excited state can be observed. The similar lifetimes of short decay components indicate that AuNPs have similar surface quenching effect for the triplet excited states of three cationic dyes. So the distinct enhancement factor exhibited for the three dyes should be related to the size and structures of AuNPs aggregation caused by different dyes, which are important factors to affect the enhancement effect.

It shows here that the strongest enhancement effect has been achieved for MB, which causes the formation of close-packed AuNPs nanoclusters consisting of 2−6 nanoparticles. Following the order of MB, azure A, thionine, the enhancement effect of nanoantennas decreases when the aggregation size increases, and the multidimensional and multilayer structures are formed. For thionine, when tens of nanoparticles are packed together, only the quenching effect on triplet excited state was observed. The enhancement effect of aggregated nanoparticles on triplet excited state formation is apparently dependent on the size and structure of aggregates. These observations can find analogue in SERS enhancement,[41] which showed that the highest enhancement factor with approximately 100 nm aggregated Ag nanoparticles will decrease if the aggregation size increases further.

Further evidence supporting the mechanism of aggregation-induced plasmon field interaction can be obtained by performing control experiments for the anionic dye, Rose Bengal (RB), as shown in Figure 4d. In contrast to cationic dyes, it is known that the anionic dyes can prevent aggregation of the citrate-stabilized AuNPs.[42,43] Because of electrostatic repulsion, the anionic dye molecules cannot be adsorbed to the surface of negatively charged AuNPs. For the triplet excited state of RB, neither enhancement nor quenching effect was observed.

CONCLUSION

In summary, we have studied the enhancement effect of AuNPs on the triplet excited state formation of three different cationic thiazine dyes and one anionic dye. For fully understanding the mechanism of this effect, we have performed well-controlled experiments of monodispersed AuNPs, in comparison with the case of aggregated AuNPs. It is found that the three cationic dyes can cause efficient aggregation of citrate-stabilized AuNPs, leading to AuNPs aggregates with varied size, whereas the ATP-protected AuNPs can be sustained in the monodispersed state. For both of the ground state absorption and triplet excited state formation of cationic dyes, the enhancement effect is only exhibited with the aggregated AuNPs, but not with the monodispersed AuNPs. The enhancement factor is shown to be largely related with the aggregation size and structure. These results suggest a mechanism of aggregation-induced plasmon field interaction of AuNPs, where AuNPs aggregates with appropriate size and structure can act as stronger plasmonic nanoantennas. While our studies have focused on triplet excited state formation upon AuNPs interaction, what we have learned may have implications for other surface-enhanced spectroscopic and energy transformation processes as well.

ASSOCIATED CONTENT

Supporting Information

Additional experimental results. This material is available free of charge via the Internet at http://pubs.acs.org.

AUTHOR INFORMATION

Corresponding Author

*E-mail: hongmei@iccas.ac.cn (H.S.).

Notes

The authors declare no competing financial interest.

ACKNOWLEDGMENTS

This work was financially supported by the National Natural Science Foundation of China (Grant 21333012) and the National Basic Research Program of China (Grant 2013CB834602). We thank Prof. Andong Xia and Dr. Tengfei Yang for helpful discussions.

REFERENCES

(1) Halas, N. J.; Lal, S.; Chang, W.-S.; Link, S.; Nordlander, P. Plasmons in Strongly Coupled Metallic Nanostructures. *Chem. Rev.* **2011**, *111*, 3913−3961.

(2) Mayer, K. M.; Hafner, J. H. Localized Surface Plasmon Resonance Sensors. *Chem. Rev.* **2011**, *111*, 3828−3857.

(3) Morton, S. M.; Silverstein, D. W.; Jensen, L. Theoretical Studies of Plasmonics Using Electronic Structure Methods. *Chem. Rev.* **2011**, *111*, 3962−3994.

(4) Barazzouk, S.; Kamat, P. V.; Hotchandani, S. Photoinduced Electron Transfer between Chlorophyll a and Gold Nanoparticles. *J. Phys. Chem. B* **2005**, *109*, 716−723.

(5) Bakhtiari, A. B. S.; Hsiao, D.; Jin, G.; Gates, B. D.; Branda, N. R. An Efficient Method Based on the Photothermal Effect for the Release of Molecules from Metal Nanoparticle Surfaces. *Angew. Chem., Int. Ed.* **2009**, *48*, 4166−4169.

(6) Fasciani, C.; Alejo, C. J. B.; Grenier, M.; Netto-Ferreira, J. C.; Scaiano, J. High-Temperature Organic Reactions at Room Temperature Using Plasmon Excitation: Decomposition of Dicumyl Peroxide. *Org. Lett.* **2010**, *13*, 204−207.

(7) Malicki, M.; Hales, J. M.; Rumi, M.; Barlow, S.; McClary, L.; Marder, S. R.; Perry, J. W. Excited-State Dynamics and Dye−Dye Interactions in Dye-Coated Gold Nanoparticles with Varying Alkyl Spacer Lengths. *Phys. Chem. Chem. Phys.* **2010**, *12*, 6267−6277.

(8) Kneipp, K.; Kneipp, H.; Kneipp, J. Surface-Enhanced Raman Scattering in Local Optical Fields of Silver and Gold Nanoaggregatess−from Single-Molecule Raman Spectroscopy to Ultrasensitive Probing in Live Cells. *Acc. Chem. Res.* **2006**, *39*, 443−450.

(9) Aroca, R. F. Plasmon Enhanced Spectroscopy. *Phys. Chem. Chem. Phys.* **2013**, *15*, 5355−5363.

(10) Fort, E.; Gresillon, S. Surface Enhanced Fluorescence. *J. Phys. D: Appl. Phys.* **2008**, *41*, 013001.

(11) Atwater, H. A.; Polman, A. Plasmonics for Improved Photovoltaic Devices. *Nat. Mater.* **2010**, *9*, 205−213.

(12) Mahmoudi, M.; Azadmanesh, K.; Shokrgozar, M. A.; Journeay, W. S.; Laurent, S. Effect of Nanoparticles on the Cell Life Cycle. *Chem. Rev.* **2011**, *111*, 3407−3432.

(13) Thomas, K. G.; Kamat, P. V. Chromophore-Functionalized Gold Nanoparticles. *Acc. Chem. Res.* **2003**, *36*, 888−898.

(14) Narband, N.; Uppal, M.; Dunnill, C. W.; Hyett, G.; Wilson, M.; Parkin, I. P. The Interaction between Gold Nanoparticles and Cationic and Anionic Dyes: Enhanced UV-Visible Absorption. *Phys. Chem. Chem. Phys.* **2009**, *11*, 10513−10518.

(15) Pacioni, N. L.; Gonzalez-Bejar, M.; Alarcon, E.; McGilvray, K. L.; Scaiano, J. C. Surface Plasmons Control the Dynamics of Excited Triplet States in the Presence of Gold Nanoparticles. *J. Am. Chem. Soc.* **2010**, *132*, 6298−6299.

(16) Steiner, M.; Debus, C.; Failla, A. V.; Meixner, A. J. Plasmon-Enhanced Emission in Gold Nanoparticle Aggregates. *J. Phys. Chem. C* **2008**, *112*, 3103−3108.
(17) Lim, S. I.; Zhong, C. J. Molecularly Mediated Processing and Assembly of Nanoparticles: Exploring the Interparticle Interactions and Structures. *Acc. Chem. Res.* **2009**, *42*, 798−808.
(18) Taylor, R. W.; Esteban, R.; Mahajan, S.; Coulston, R.; Scherman, O. A.; Aizpunia, J.; Baumberg, J. J. Simple Composite Dipole Model for the Optical Modes of Strongly-Coupled Plasmonic Nanoparticle Aggregates. *J. Phys. Chem. C* **2012**, *116*, 25044−25051.
(19) Sanchot, A.; Baffou, G.; Marty, R.; Arbouet, A.; Quidant, R.; Girard, C.; Dujardin, E. Plasmonic Nanoparticle Networks for Light and Heat Concentration. *ACS Nano* **2012**, *6*, 3434−3440.
(20) Keene, A. M.; Tyner, K. M. Analytical Characterization of Gold Nanoparticle Primary Particles, Aggregates, Agglomerates, and Agglomerated Aggregates. *J. Nanopart. Res.* **2011**, *13*, 3465−3481.
(21) Shegai, T.; Brian, B.; Miljkovic, V. D.; Kall, M. Angular Distribution of Surface-Enhanced Raman Scattering from Individual Au Nanoparticle Aggregates. *ACS Nano* **2011**, *5*, 2036−2041.
(22) Wang, Y. F.; Zeiri, O.; Neyman, A.; Stellacci, F.; Weinstock, I. A. Nucleation and Island Growth of Alkanethiolate Ligand Domains on Gold Nanoparticles. *ACS Nano* **2012**, *6*, 629−640.
(23) Enustun, B. V.; Turkevich, J. Coagulation of Colloidal Gold. *J. Am. Chem. Soc.* **1963**, *85*, 3317−3328.
(24) Frens, G. Controlled Nucleation for Regulation of Particle-Size in Monodisperse Gold Suspensions. *Nat. Phys. Sci.* **1973**, *241*, 20−22.
(25) Yang, C.; Yu, Y.; Liu, K.; Song, D.; Wu, L.; Su, H. 2 + 2 Photocycloaddition Reaction Dynamics of Triplet Pyrimidines. *J. Phys. Chem. A* **2011**, *115*, 5335−5345.
(26) Wang, H.; He, Y.; Li, Y.; Su, H. Photophysical and Electronic Properties of Five Pcbm-Like C-60 Derivatives: Spectral and Quantum Chemical View. *J. Phys. Chem. A* **2012**, *116*, 255−262.
(27) Chandrasekharan, N.; Kamat, P. V.; Hu, J. Q.; Jones, G. Dye-Capped Gold Nanoclusters: Photoinduced Morphological Changes in Gold/Rhodamine 6G Nanoassemblies. *J. Phys. Chem. B* **2000**, *104*, 11103−11109.
(28) Ding, Y. H.; Chen, Z. Q.; Xie, J.; Guo, R. Comparative Studies on Adsorption Behavior of Thionine on Gold Nanoparticles with Different Sizes. *J. Colloid Interface Sci.* **2008**, *327*, 243−250.
(29) Chegel, V.; Rachkov, O.; Lopatynskyi, A.; Ishihara, S.; Yanchuk, I.; Nemoto, Y.; Hill, J. P.; Ariga, K. Gold Nanoparticles Aggregation: Drastic Effect of Cooperative Functionalities in a Single Molecular Conjugate. *J. Phys. Chem. C* **2012**, *116*, 2683−2690.
(30) Bellino, M. G.; Calvo, E. J.; Gordillo, G. Adsorption Kinetics of Charged Thiols on Gold Nanoparticles. *Phys. Chem. Chem. Phys.* **2004**, *6*, 424−428.
(31) Wang, G.; Sun, W. Optical Limiting of Gold Nanoparticle Aggregates Induced by Electrolytes. *J. Phys. Chem. B* **2006**, *110*, 20901−20905.
(32) Bharadwaj, P.; Novotny, L. Spectral Dependence of Single Molecule Fluorescence Enhancement. *Opt. Express* **2007**, *15*, 14266−14274.
(33) Park, Q. H. Optical Antennas and Plasmonics. *Contemp. Phys.* **2009**, *50*, 407−423.
(34) Zhao, W.; Gonzaga, F.; Li, Y.; Brook, M. A. Highly Stabilized Nucleotide-Capped Small Gold Nanoparticles with Tunable Size. *Adv. Mater.* **2007**, *19*, 1766−1771.
(35) Zhao, W.; Lee, T. M. H.; Leung, S. S. Y.; Hsing, I. M. Tunable Stabilization of Gold Nanoparticles in Aqueous Solutions by Mononucleotides. *Langmuir* **2007**, *23*, 7143−7147.
(36) Zhao, W.; Chiuman, W.; Lam, J. C. F.; Brook, M. A.; Li, Y. Simple and Rapid Colorimetric Enzyme Sensing Assays Using Non-Crosslinking Gold Nanoparticle Aggregation. *Chem. Commun.* **2007**, *36*, 3729−3731.
(37) Chang, W. S.; Willingham, B.; Slaughter, L. S.; Dominguez-Medina, S.; Swanglap, P.; Link, S. Radiative and Nonradiative Properties of Single Plasmonic Nanoparticles and Their Assemblies. *Acc. Chem. Res.* **2012**, *45*, 1936−1945.
(38) Maier, S. A.; Kik, P. G.; Atwater, H. A.; Meltzer, S.; Harel, E.; Koel, B. E.; Requicha, A. A. G. Local Detection of Electromagnetic Energy Transport below the Diffraction Limit in Metal Nanoparticle Plasmon Waveguides. *Nat. Mater.* **2003**, *2*, 229−232.
(39) Kleinman, S. L.; Sharma, B.; Blaber, M. G.; Henry, A.-I.; Valley, N.; Freeman, R. G.; Natan, M. J.; Schatz, G. C.; Van Duyne, R. P. Structure Enhancement Factor Relationships in Single Gold Nanoantennas by Surface-Enhanced Raman Excitation Spectroscopy. *J. Am. Chem. Soc.* **2012**, *135*, 301−308.
(40) Acuna, G.; Möller, F.; Holzmeister, P.; Beater, S.; Lalkens, B.; Tinnefeld, P. Fluorescence Enhancement at Docking Sites of DNA-Directed Self-Assembled Nanoantennas. *Science* **2012**, *338*, 506−510.
(41) Sun, L. L.; Zhao, D. X.; Ding, M.; Xu, Z. K.; Zhang, Z. Z.; Li, B. H.; Shen, D. Z. Controllable Synthesis of Silver Nanoparticle Aggregates for Surface-Enhanced Raman Scattering Studies. *J. Phys. Chem. C* **2011**, *115*, 16295−16304.
(42) Wiederrecht, G. P.; Wurtz, G. A.; Hranisavljevic, J. Coherent Coupling of Molecular Excitons to Electronic Polarizations of Noble Metal Nanoparticles. *Nano Lett.* **2004**, *4*, 2121−2125.
(43) Blakey, I.; Schiller, T. L.; Merican, Z.; Fredericks, P. M. Interactions of Phenyldithioesters with Gold Nanoparticles (AuNPs): Implications for AuNP Functionalization and Molecular Barcoding of AuNP Assemblies. *Langmuir* **2010**, *26*, 692−701.